

Phase equilibria in the Sm–Co–Sn ternary system at 870 K and 770 K

L. ROMAKA^{1*}, V.V. ROMAKA¹, M. KONYK¹, N. MELNYCHENKO-KOBYLYUK¹

¹ Department of Inorganic Chemistry, Ivan Franko National University of Lviv,
Kyryla i Mefodiya St. 6, 79005 Lviv, Ukraine

* Corresponding author. E-mail: romakal@franko.lviv.ua

Received February 27, 2008; accepted June 18, 2008; available on-line September 10, 2008

The phase diagram of the Sm–Co–Sn ternary system was constructed at 770 K (more than 55 at.% Sn) and 870 K (0–55 at.% Sn) using X-ray and metallographic analyses. Seven ternary intermetallic compounds, $\text{Sm}_3\text{Co}_8\text{Sn}_4$ ($\text{Lu}_3\text{Co}_{7.77}\text{Sn}_4$ -type), $\text{Sm}_6\text{Co}_2\text{Sn}$ ($\text{Ho}_6\text{Co}_2\text{Ga}$ -type), $\text{Sm}_{12}\text{Co}_6\text{Sn}$ ($\text{Sm}_{12}\text{Ni}_6\text{In}$ -type), $\text{Sm}_3\text{Co}_6\text{Sn}_5$ ($\text{Dy}_3\text{Co}_6\text{Sn}_5$ -type), Sm_2CoSn_2 (related to the $\text{Tb}_{117}\text{Fe}_{52}\text{Ge}_{112}$ -type), $\text{SmCo}_{1-x}\text{Sn}_{2-y}$ (CeNiSi_2 -type), and $\text{Sm}_6\text{Co}_8\text{Sn}_{26}$ ($\text{Yb}_6\text{Rh}_8\text{Sn}_{26}$ -type), are formed in this system at the investigated temperatures.

Intermetallics / X-ray diffraction / Phase diagrams / Crystal structure

1. Introduction

The results of systematic investigations of the interaction between the components in R – Me – Sn systems (R – rare earth, Me – 3d-element), the composition, crystal structure and physical properties of the ternary stannides are discussed by Skolozdra in [1]. The study of the magnetic properties of ternary intermetallic phases containing a rare earth and a magnetic transition element such as iron or cobalt is the principal orientation in the search for new materials suitable for permanent-magnet fabrication. In this context the investigation of the R – Co – Sn ternary systems is very interesting, in particular the synthesis, crystal structure of the compounds and phase equilibria. The Co-containing ternary systems with rare-earth metals and tin have so far not been systematically studied. Isothermal sections have been constructed completely only for the Er–Co–Sn [2] and Nd–Co–Sn [3] systems. Information about investigations of the systems with $R = \text{Y}, \text{Ce}, \text{Gd}$ and Lu was presented in [1].

Preliminary results of an investigation of the Sm–Co–Sn ternary system at 770 K (0–50 at.% Sn) and 670 K (up to 50 at.% Sn) including the formation of seven ternary compounds ($\text{Sm}_6\text{Co}_8\text{Sn}_{26}$, $\text{SmCo}_{1-x}\text{Sn}_{2-y}$, $\text{Sm}_6\text{Co}_2\text{Sn}$, SmCo_3Sn , $\text{Sm}_4\text{Co}_3\text{Sn}_3$, SmCo_2Sn_2 , and $\text{Sm}_{65}\text{Co}_{25}\text{Sn}_{10}$) were reported in [1], but the phase equilibria were not determined. The other R – Co – Sn ternary systems have been studied in part during investigations of series of isostructural compounds.

In this paper we present the results of an X-ray investigation of the phase equilibria in the Sm–Co–Sn

ternary system at 770 and 870 K and crystal structure data for the ternary compounds.

2. Binary boundary systems

The binary boundary systems that delimit the ternary Sm–Co–Sn system have been investigated earlier; the binary compounds formed in these systems are briefly described below.

Sm–Sn system

Data concerning the phase diagram and crystallographic characteristics of the binaries of the Sm–Sn system were assessed in Massalski's compilation [4]. Seven binary compounds are formed in this system: SmSn_3 (Cu_3Au structure type (ST)), SmSn_2 (ZrGa_2 ST), Sm_2Sn_3 (own ST), $\text{Sm}_{11}\text{Sn}_{10}$ ($\text{Ho}_{11}\text{Ge}_{10}$ ST), Sm_5Sn_4 (Sm_5Ge_4 ST), Sm_4Sn_3 (Th_3P_4 ST), Sm_5Sn_3 (Mn_5Si_3 ST). The $\text{Sm}_{11}\text{Sn}_{10}$ phase exists in a small temperature range above 1440 K. Crystal structure investigations of the new binaries Sm_2Sn_5 (Ce_2Sn_5 ST) and Sm_3Sn_7 (Tb_3Sn_7 ST), were reported by Weitzer *et al.* in [5].

Sm–Co system

Seven binary phases were observed at 870 K in the Sm–Co phase diagram according to Massalski [4] and Villars and Calvert [6]: $\text{Sm}_2\text{Co}_{17}$ ($\text{Th}_2\text{Ni}_{17}$ ST), SmCo_5 (CaCu_5 ST), Sm_2Co_7 (Gd_2Co_7 ST), SmCo_3 (PuNi_3 ST), SmCo_2 (MgCu_2 ST), Sm_5Co_2 (Mn_5C_2 ST), and Sm_3Co (Fe_3C ST). The $\text{Sm}_5\text{Co}_{19}$ compound ($\text{Sm}_5\text{Co}_{19}$ ST) exists above 1473 K.

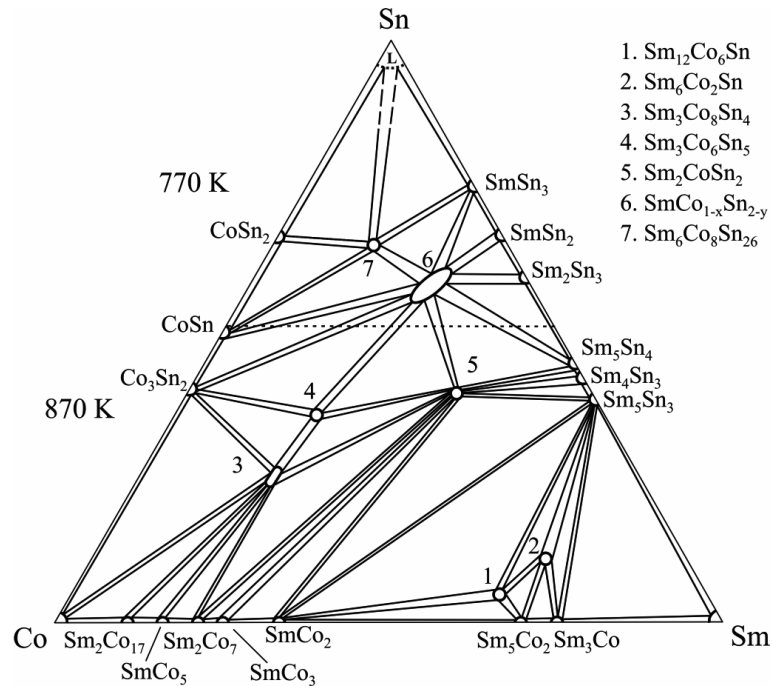


Fig. 1 Isothermal sections for the Sm–Co–Sn system at 870 K (0–55 at.% Sn) and 770 K (more than 55 at.% Sn).

Co–Sn system

The version of this well studied phase diagram used in our investigation was taken from Massalski [4] and Villars and Calvert [6]. At 770 and 870 K only three phases are observed: Co_3Sn_2 (Ni_3Sn_2 *ST*), CoSn (own *ST*), and CoSn_2 (CuAl_2 *ST*). Data for the new binaries α - CoSn_3 (PdSn_3 *ST*) and β - CoSn_3 (own *ST*) was reported in [7].

3. Experimental

The samples were prepared by direct arc melting of the constituent elements (Sm, purity 99.9 wt.%, Co 99.99 wt.%, and Sn 99.999 wt.%) under purified, Ti-gettered, argon atmosphere, with a non-consumable tungsten electrode, on a water-cooled copper hearth. The overall weight losses were generally less than 1 wt.%. The alloys were annealed at 870 K (0–55 at.% Sn) and 770 K (more than 55 at.% Sn) in evacuated quartz tubes for 1400 hours and subsequently quenched in ice water.

X-ray analysis was the main method for the construction of the isothermal section. It was carried out using the Debye-Scherrer method and powder patterns obtained on DRON-2.0m ($\text{Fe } K_\alpha$ radiation) and Philips PW1720 ($\text{Cu } K_\alpha$ radiation) powder diffractometers. The observed intensities were compared with reference powder patterns of known binary and ternary phases. For the crystal structure refinements, powder patterns obtained on Guinier image plate ($\text{Cu } K_\alpha$ radiation, 2θ scanning in the range

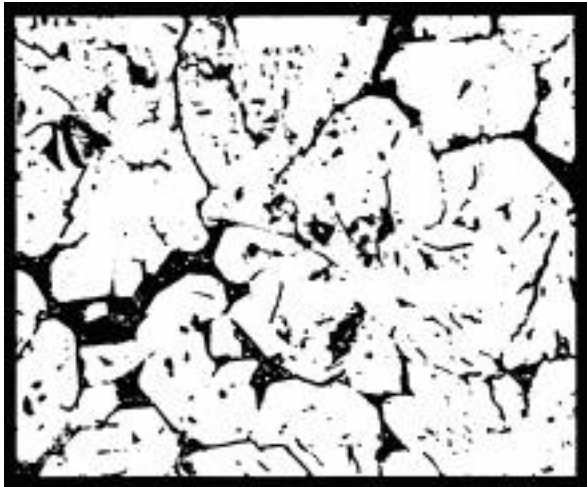
8–100°, in transmission mode) and Siemens D5000 automatic diffractometers ($\text{Cu } K_\alpha$ radiation) were used. The theoretical patterns and the crystal structure parameters were calculated using the CSD [8] and WinPLOTR [9] program packages.

The phase purity and final sample composition of some of the alloys were controlled by X-ray powder diffraction using automatic diffractometers or by Electron Probe Micro-Analysis (EPMA) on a Carl Zeiss DSM 962 equipped with a Link EDX system operating at 20 kV and 60 mA.

4. Results and discussion

The phase diagram of the Sm–Co–Sn ternary system at 870 K (0–55 at.% Sn) and 770 K (more than 55 at.% Sn) was constructed based on X-ray and partial metallographic analyses of 167 ternary and 15 binary alloys (Fig. 1). The annealing temperature 870 K was preferred for the alloys with higher Co content because the diffraction patterns obtained from the samples annealed at this temperature were of better quality. The presence of almost all binary compounds reported in the literature for the Sm–Co, Sm–Sn and Co–Sn systems was confirmed. Due to the chemical activity of the alloys in the range 40–60 at.% Sn there were some difficulties with the syntheses of the Sm_5Sn_4 , and Sm_4Sn_3 compounds. Diffraction peaks corresponding to these compounds were present in films of ternary and binary alloys in concentration regions close to the stoichiometric composition of

these phases. Microphotographs of some ternary alloys are reported in Figs. 2 and 3.



(a)

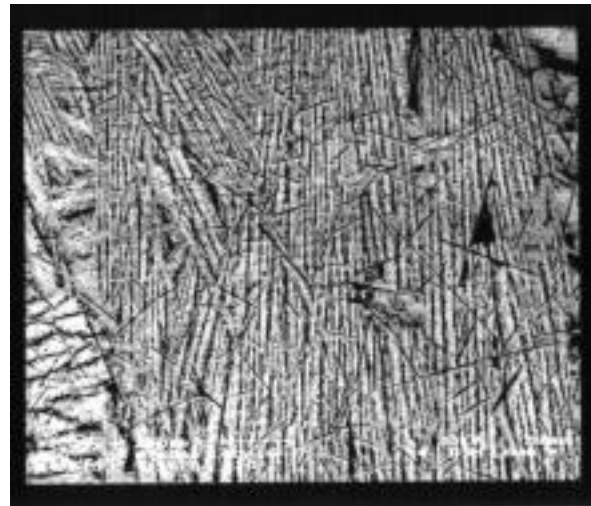


(b)

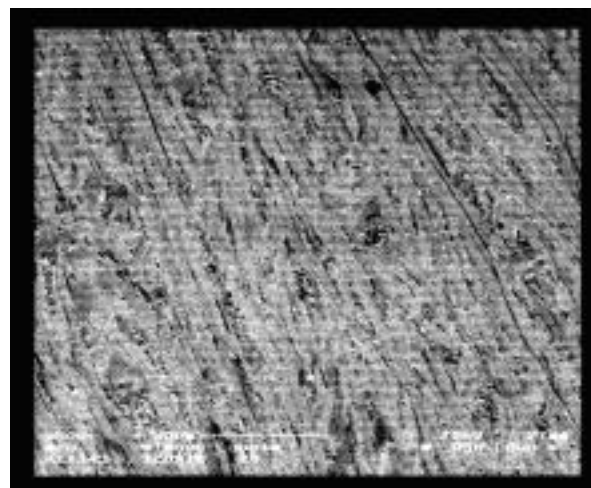
Fig. 2 Electron micrograph of the alloys (a) $\text{Sm}_{35}\text{Co}_{30}\text{Sn}_{35}$ (white phase – $\text{Sm}_{40}\text{Co}_{20}\text{Sn}_{40}$; black phase – $\text{Sm}_3\text{Co}_8\text{Sn}_4$) and (b) $\text{Sm}_{45}\text{Co}_{10}\text{Sn}_{45}$ (white phase – Sm_5Sn_4 ; black phase – $\text{Sm}_{40}\text{Co}_{20}\text{Sn}_{40}$).

The phase equilibria in the Sm–Co–Sn ternary system are characterized by the formation of seven ternary compounds at the investigated temperatures. The crystallographic characteristics of the compounds $\text{SmCo}_{1-x}\text{Sn}_{2-y}$ (CeNiSi_2 ST), $\text{Sm}_6\text{Co}_8\text{Sn}_{26}$ ($\text{Yb}_6\text{Rh}_8\text{Sn}_{26}$ ST) [1], $\text{Sm}_3\text{Co}_6\text{Sn}_5$ ($\text{Dy}_3\text{Co}_6\text{Sn}_5$ ST) [10] and $\text{Sm}_3\text{Co}_8\text{Sn}_4$ ($\text{Lu}_3\text{Co}_{7.77}\text{Sn}_4$ ST) were confirmed and the crystal structures of the three other ternary stannides were determined. A preliminary investigation of the ternary phase found at the composition $\text{Sm}_{20}\text{Co}_{60}\text{Sn}_{20}$ showed that it belongs to the BaLi_4 type of structure

[11]. Further studies performed in [12] allowed to determine the $\text{Lu}_3\text{Co}_{7.77}\text{Sn}_4$ structure type (an ordered, non-centrosymmetric variant of the BaLi_4 type with full occupancy of all atomic positions) and the formula $\text{Sm}_3\text{Co}_8\text{Sn}_4$. A detailed investigation of samples in this region showed a small homogeneity range for the $\text{Sm}_3\text{Co}_8\text{Sn}_4$ compound of about 3 at.% along the isoconcentrate of samarium, the lattice parameters changing from $a = 0.8923(7)$, $c = 0.7543(8)$ nm (for $\text{Sm}_{20}\text{Co}_{56}\text{Sn}_{24}$) to $a = 0.8938(2)$, $c = 0.7549(3)$ nm (for $\text{Sm}_{20}\text{Co}_{53}\text{Sn}_{27}$). It is worth noting the absence of an equiatomic SmCoSn compound. As confirmed by the X-ray and metallographic analyses, the sample $\text{Sm}_{35}\text{Co}_{30}\text{Sn}_{35}$ contained two phases: $\text{Sm}_3\text{Co}_8\text{Sn}_4$ and Sm_2CoSn_2 (Fig. 2a). The crystallographic characteristics of the compounds formed in the Sm–Co–Sn ternary system are presented in Table 1.



(a)



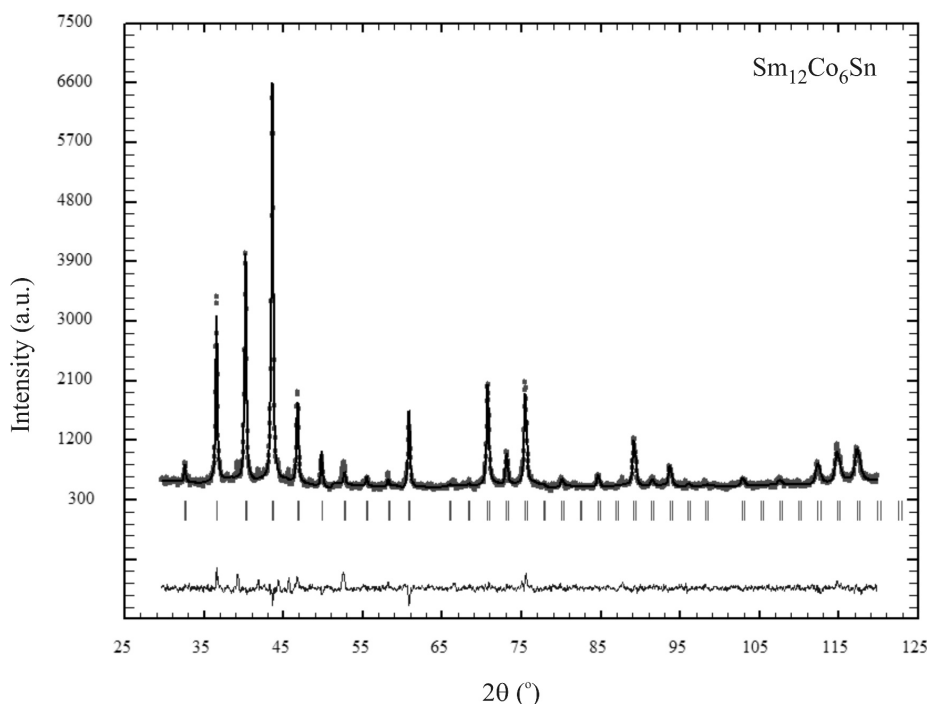
(b)

Fig. 3 Electron micrograph of the alloys (a) $\text{Sm}_{15}\text{Co}_{25}\text{Sn}_{60}$ (gray phase – $\text{Sm}_6\text{Co}_8\text{Sn}_{26}$; black phase – CoSn) and (b) $\text{Sm}_{25}\text{Co}_{30}\text{Sn}_{45}$ (light gray phase – $\text{Sm}_3\text{Co}_6\text{Sn}_5$; dark gray phase – $\text{Sm}_{30}\text{Co}_{14}\text{Sn}_{56}$).

Table 1 Crystallographic data for the ternary compounds of the Sm–Co–Sn system.

#	Compound	Structure type	Space group	Unit cell parameters, nm		
				<i>a</i>	<i>b</i>	<i>c</i>
1	Sm ₁₂ Co ₆ Sn	Sm ₁₂ Ni ₆ In	<i>Im-3</i>	0.9754(2)		
2	Sm ₆ Co ₂ Sn	Ho ₆ Co ₂ Ga	<i>Immm</i>	0.9268(7)	0.9285(7)	0.9839(9)
3	Sm ₃ Co ₈ Sn ₄	Lu ₃ Co _{7.77} Sn ₄	<i>P6₃mc</i>	0.8938(2)		0.7549(3)
4	Sm ₃ Co ₆ Sn ₅	Dy ₃ Co ₆ Sn ₅	<i>Immm</i>	0.4321(2)	1.2470(4)	0.9778(3)
5	Sm ₂ CoSn ₂	related to Tb ₁₁₇ Fe ₅₂ Ge ₁₁₂	<i>Fm-3m</i>	3.1968(6)		
6	SmCo _{0.39} Sn _{1.84}	CeNiSi ₂	<i>Cmcm</i>	0.4469(2)	1.667(1)	0.4449(2)
7	Sm ₆ Co ₈ Sn ₂₆	Yb ₆ Rh ₈ Sn ₂₆	<i>Pm-3n</i>	0.9524(3)		

The compound number corresponds to the figure in the phase diagram (Fig. 1)

**Fig. 4** The observed, calculated and difference X-ray patterns of the Sm₆₅Co₃₀Sn₅ sample.

In the samarium-rich region of the Sm–Co–Sn ternary system the formation of two ternary compounds, Sm₁₂Co₆Sn and Sm₆Co₂Sn, was observed. The crystal structure refinement of the Sm₁₂Co₆Sn compound was performed by the Rietveld method on the Sm₆₅Co₃₀Sn₅ sample. Sm₁₂Co₆Sn crystallizes with the Sm₁₂Ni₆In structure type (space group (*SG*) *Im-3*, *a* = 0.97542(3) nm) with the final atom coordinates: Sm in 24(*g*) 0 *y* *z* (*y* = 0.1918(4), *z* = 0.6989(3)); Co in 12(*e*) *x* 0 ½ (*x* = 0.1085(7)); Sn in 2(*a*) 0 0 0 (*R_p* = 0.040, *R_{wp}* = 0.054, *R_{Bragg}* = 0.052). The cubic unit cell contains 24 samarium atoms occupying a site of relatively low symmetry. The observed, calculated and difference X-ray patterns of the Sm₆₅Co₃₀Sn₅ sample are shown in Fig. 4.

The reflections of the powder pattern of the Sm₆₅Co₂₄Sn₁₁ sample were indexed on the basis of an orthorhombic lattice with cell parameters *a* = 0.9268(7), *b* = 0.9285(7), *c* = 0.9839(9) nm. The

analysis of the *hkl* indices of the reflections, their intensity, and the lattice parameters indicate a probable relation to the Ho₆Co₂Ga structure type (*SG Immm*). The phase analysis of the powder pattern of the corresponding ingot showed a small presence of Sm₅Sn₃ (Mn₅Si₃ *ST*) as impurity phase, which was taken into account during the crystal structure calculations. The atoms occupy the following positions: Sm1 in 8(*n*) *x* *y* 0 (*x* = 0.28765(4), *y* = 0.18519(4)); Sm2 in 8(*m*) *x* 0 *z* (*x* = 0.31007(4), *z* = 0.31649(3)); Sm3 in 8(*l*) 0 *y* *z* (*y* = 0.19380(5), *z* = 0.21480(3)); Co1 in 4(*j*) ½ 0 *z* (*z* = 0.10803(1)); Co2 in 4(*g*) 0 *y* 0 (*y* = 0.38145(1)); Sn1 in 2(*c*) ½ ½ 0; Sn2 in 2(*a*) 0 0 0 (*R_p* = 0.013, *R_{wp}* = 0.017, *R_{Bragg}* = 0.109). The observed, calculated and difference X-ray patterns of the Sm₆₅Co₂₄Sn₁₁ sample are shown in Fig. 5. The Sm₆Co₂Sn compound is isostructural to the series of the previously studied R₆Co₂Sn stannides (*R* = Gd–Lu), which form in the

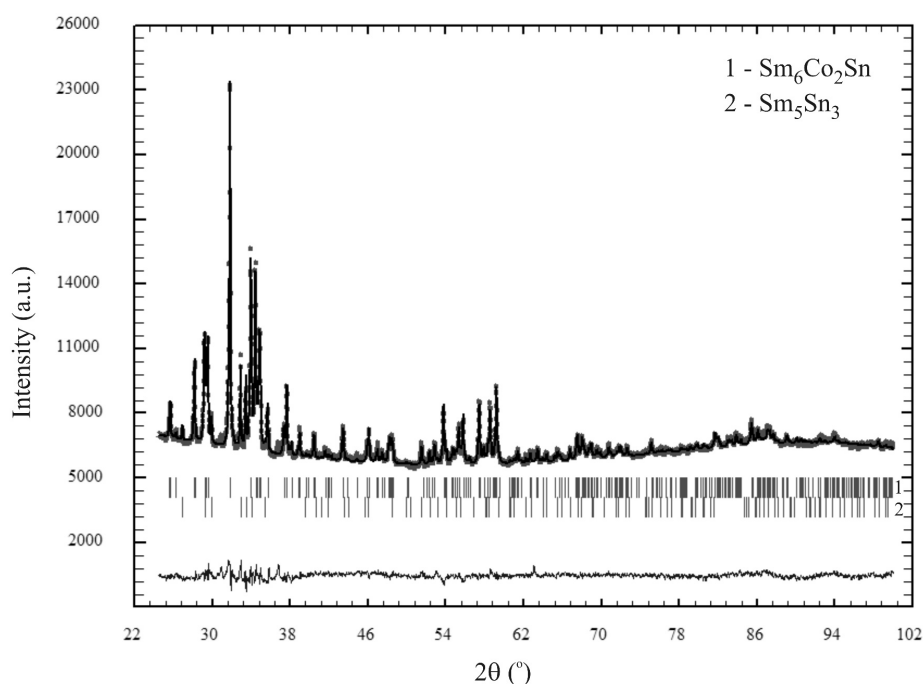


Fig. 5 The observed, calculated and difference X-ray patterns of the $\text{Sm}_{65}\text{Co}_{24}\text{Sn}_{11}$ sample.

R–Co–Sn systems and crystallize in the $\text{Ho}_6\text{Co}_2\text{Ga}$ structure type. The structures of the $\text{Sm}_{12}\text{Co}_6\text{Sn}$ and $\text{Sm}_6\text{Co}_2\text{Sn}$ compounds are related and characterized by antiprismatic-tetragonal coordination of the Co atoms. The interatomic distances (δ) do not show any significant deviation from the sum of the atomic radii of the corresponding components, except for the shortest distances between cobalt atoms (Co–Co ($\delta = 0.212$ nm) for $\text{Sm}_{12}\text{Co}_6\text{Sn}$; Co1–Co1 ($\delta = 0.213$ nm), and Co2–Co2 ($\delta = 0.220$ nm) for $\text{Sm}_6\text{Co}_2\text{Sn}$).

The formation of a new family of $R_2\text{CoSn}_2$ compounds ($R = \text{La}–\text{Sm}$), probably related to the $\text{Tb}_{117}\text{Fe}_{52}\text{Ge}_{112}$ -type with a very large face-centered cubic cell, was reported in [13]. The existence of the Sm_2CoSn_2 stannide with the lattice parameter $a = 3.1968(6)$ nm was confirmed by X-ray and partial metallographic analyses during our investigation.

X-ray analysis has confirmed the formation of the $\text{SmCo}_{1-x}\text{Sn}_{2-y}$ ternary phase crystallizing in the CeNiSi_2 structure type [14,15,16]. The homogeneity range at 770 K is limited by the compositions $\text{SmCo}_{0.46}\text{Sn}_{1.86}$ and $\text{SmCo}_{0.39}\text{Sn}_{1.84}$, while the stoichiometric SmCoSn_2 composition is not included in the concentration range. It is worth noting that numerous investigations of $R\text{Me}_{1-x}\text{Sn}_{2-y}$ phases ($\text{Me} = \text{Mn}, \text{Fe}, \text{Co}, \text{Ni}, \text{Cu}$) with CeNiSi_2 -type have shown that the structure has defects in the atomic positions of the 3*d*-metal and Sn, the amount of defects depending on the rare earth and 3*d*-elements. An investigation of the composition of the SmCo_xSn_2 phase performed along the

SmSn_2 – SmCoSn_2 line at 1073 K [16] showed the formation of $\text{SmCo}_{0.38}\text{Sn}_2$ with defects in the Co position. A detailed study of the corresponding ternary region of the Sm–Co–Sn system allowed us to determine the homogeneity range of the $\text{SmCo}_{1-x}\text{Sn}_{2-y}$ phase at 770 K. The results are in a good agreement with [1] and with the previously studied Nd–Co–Sn system [3].

No solid solution ranges were observed for the binary compounds in the Sm–Co–Sn system at the investigated temperatures.

The character of the phase relations, compositions and crystal structures of the ternary compounds formed in the Sm–Co–Sn system show a great similarity with the previously studied Nd–Co–Sn system. $R\text{CoSn}$ (TiNiSi *ST*) and $R_7\text{Co}_6\text{Sn}_{23}$ ($\text{Ho}_7\text{Co}_6\text{Sn}_{23}$ *ST*) compounds have only been observed for heavy rare-earth intermetallic systems (Er–Co–Sn system).

Acknowledgements

This work was supported by the Ukrainian Ministry of Education and Science (Grant 010U001299).

References

- [1] R.V. Skolozdra, Stannides of rare earth and transition metals, in: K.A. Gschneidner Jr.,

- L. Eyring (Eds.), *Handbook on the Physics and Chemistry of Rare Earths*, Vol. 24, 1997, 399-557.
- [2] R.V. Skolozdra, Ya.S. Mudryk, L.P. Romaka, *J. Alloys Compd.* 296 (2000) 290-292.
- [3] V. Babyuk, O. Bodak, L. Romaka, A. Tkachuk, Yu. Gorelenko, *J. Alloys Compd.* 441 (2007) 107-110.
- [4] T.B. Massalski, *Binary Alloy Phase Diagrams*, ASM, Metals Park, OH, 1990.
- [5] F. Weitzer, K. Hiebl, P. Rogl, *J. Solid State Chem.* 98 (1992) 291-300.
- [6] P. Villars, L.D. Calvert, *Pearson's Handbook of Crystallographic Data for Intermetallic Phases*, ASM, Metals Park, OH, 1991.
- [7] A. Lang, W. Jeitschko, *Z. Metallkd.* 87 (1996) 759-764.
- [8] L.G. Akselrud, Yu.N. Grin, P.Yu. Zavalii, V.K. Pecharsky, V.S. Fundamenskii, CSD - universal program package for single crystal or powder structure data treatment, *Coll. Abstr. 12th Eur. Crystallogr. Meet.*, Nauka, Moscow, 1989, Vol. 3, p. 155.
- [9] J. Rodriguez-Carvajal, *FULLPROF: A Program for Rietveld Refinement and Pattern Matching Analysis*, version 3.5d, Laboratoire Léon Brillouin (CEA–CNRS), Saclay, France, 1998.
- [10] R. Pöttgen, *J. Alloys Compd.* 224 (1995) 14-17.
- [11] J. Mudryk, D. Fruchart, D. Gignoux, L.P. Romaka, R.V. Skolozdra, *J. Alloys Compd.* 312 (2000) 9-11.
- [12] F. Canepa, S. Cirafici, M.L. Fornasini, P. Manfrinetti, F. Merlo, A. Palenzona, M. Pani, *J. Alloys Compd.* 297 (2000) 109-113.
- [13] S. Cirafici, F. Canepa, P. Manfrinetti, M. Napoletano, *J. Alloys Compd.* 317-318 (2001) 550-555.
- [14] R.V. Skolozdra, *Stannides of Rare Earth and Transition Metals*, Svit, Lviv, Ukraine, 1993, 200 pp.
- [15] R.V. Skolozdra, Yu.K. Gorelenko, E.E. Terletskaia, V.D. Tkachuk, *Fiz. Met. Metalloved.* 66 (1988) 864-870.
- [16] M. François, G. Venturini, B. Malaman, B.J. Roques, *J. Less-Common Met.* 160 (1990). 197-213.